Yijie Zhang[1]
Juhong Jia[2*]

Study on the Solar Radiation and Heat Transfer of Cabin Fabric Using the Finite Volume Method

DOI: 10.5604/01.3001.0014.6080

[1] **Shaoxing University, Shangyu College,**
Shaoxing, Zhejiang 312300, China,
e-mail: zyijie@usx.edu.cn

[2] **School of Aerospace Engineering, Beijing Institute of Technology,**
Beijing 100081, China
* e-mail: jiajuhongbit@126.com

Abstract
The heat transfer of different fabrics was investigated numerically in the cabin of an aircraft. The discrete ordinate (DO) radiation model was adopted to describe the solar radiation through the cabin window and the fabric's reflection. The conjugate heat transfer between the air flow and the seat fabric was included to study the influence of the textile type and fabric thickness. Some important parameters such as the temperature, radiative heat flux, and heat transfer coefficient on the fabric surface were evaluated. The results showed that both altering of the textile type and thickness will bring about the variation of temperature on the cushion surface. The carbon fibre yarn seat and thinner padding fabric provide a much more enjoyable environment than others. The air circulation in the cabin can improves the thermal environment to some degree.

Key words: *cabin textile, heat transfer, solar radiation, thermal comfort, numerical simulation.*

Nomenclature

Q	*heat flux on vehicle surface*
P	*static pressure*
Ma	*Mach number*
T	*temperature*
T_{wall}	*temperature on wall surface*
T_∞	*inflow temperature*
Nu	*Nusselt numbers*
ϑ	*thermal capacitance*
K	*thermal conductivity*
L	*reference length*
H	*fabric thickness*
v_∞	*inflow velocity*
ρ	*bulk density*
C_p	*specific heat at constant pressure*
St	*dimensionless heat flux coefficient*
I_p	*equivalent emission of the particles*
κ_p	*equivalent absorption coefficient*
γ_p	*equivalent scattering coefficient*
N_i	*number density*
ε_{pi}	*emissivity*
d_i	*particle diameter*
T_{pi}	*particle temperature*
A_{pi}	*projected area*
α_{pi}	*particle scattering factor*

Introduction

The development of science and technology has brought about higher demands in flight comfort. One of the important parts of flight comfort is the individual seat climate, which may informally be called "thermal comfort". The thermal comfort of passengers in the cabin is related to relevant boundary conditions, such as the inlet flow, solar radiation and heat dissipation capacity of the cabin seat [1, 2]. As such, the material and thickness of the seat fabric need to be sensitive enough to the environment and generate a reasonable thermal microenvironment in the aircraft cabin.

Many numerical and experimental studies have been carried out on the heat and mass transfer involved in the internal fluid flow in aircraft cabins. Hatch [3] argued that fabric structural features, not component fibres, are the most important controllers of thermal dissipation. Bhattacharjee [4] studied the heat transfer coefficient of fabric under natural and force heat convection numerically, and found that the values from numerical simulation had good agreement with the experimental data. Günther et al. [5] investigated the airflow in an aircraft cabin using a combination of numerical simulation and experimentation by particle image velocimetry (PIV). Kühn et al. [6] discussed the forced and mixed convection as well as the received temperature field in the cabin mock-up of a passenger aircraft using PIV. Hu [7] studied the heat transfer in an aircraft cabin in various inlet conditions. But he considered the thermal radiation along the solid walls in the cabin as negligible. Maier [8] analysed the thermal comfort of ceiling-based cabin displacement ventilation and argued that more homogeneous cabin air flow was found in the mixture of the cabin displacement ventilation and ceiling-based cabin displacement ventilation methods. Khalil [9] considered the airflow and airborne pathogen transport in aircraft cabins.

As noted above, the exchange of heat in an aircraft cabin follows a distinct phenomenon of simultaneous conduction, convection, and radiation. The solar radiation and conjugate heat transfer through the fabric is difficult to model as the mechanism is very complex and there is limited research work in this area [10, 11]. With the purpose of investigating the natural and forced convection as well as solar radiation in a cabin, and studying the influence of textile type and fabric thickness, the computational fluid dynamics (CFD) method coupled with the discrete ordinate (DO) radiation model is used to predict the heat transfer and temperature distribution in an aircraft cabin. The main objectives of the present study are (1) the heat transfer and temperature distribution property and its mechanism, (2) visualisation of the cabin air flow because of forced air circulation and natural convection due to buoyancy effects, and (3) the influence of the seat fabric and thickness.

Physical model and numerical method

Heat transfer phenomenon in aircraft cabin

In real conditions, the cabin–fabric–environment system under heat convection and radiation is very complicated. The typical solar radiation and heat transfer mechanism in an air cabin is described in ***Figure 1*** approximately. When an aircraft cruises at high attitude, solar radiation becomes a fierce problem that needs to be considered. When solar rays pass through the cabin glass porthole at an inclined angle, the solar radiation

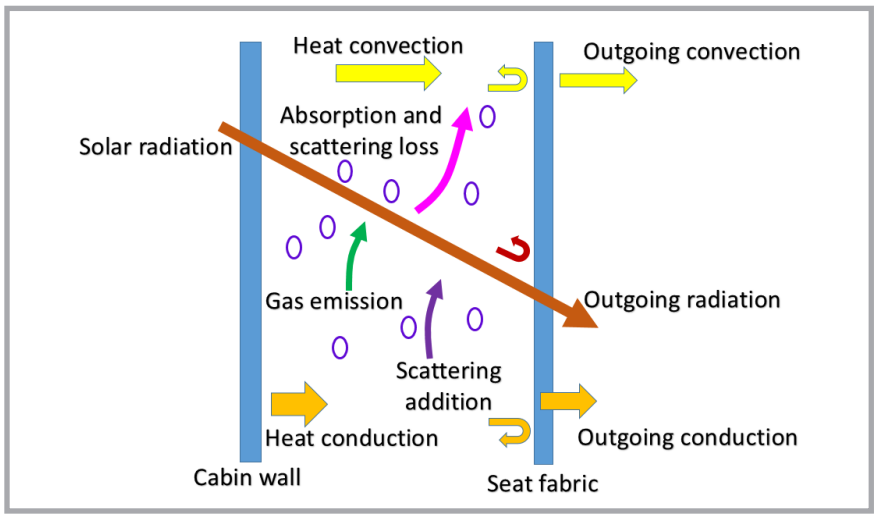

Figure 1. *Schematic of heat conduction, convection and radiation phenomenon.*

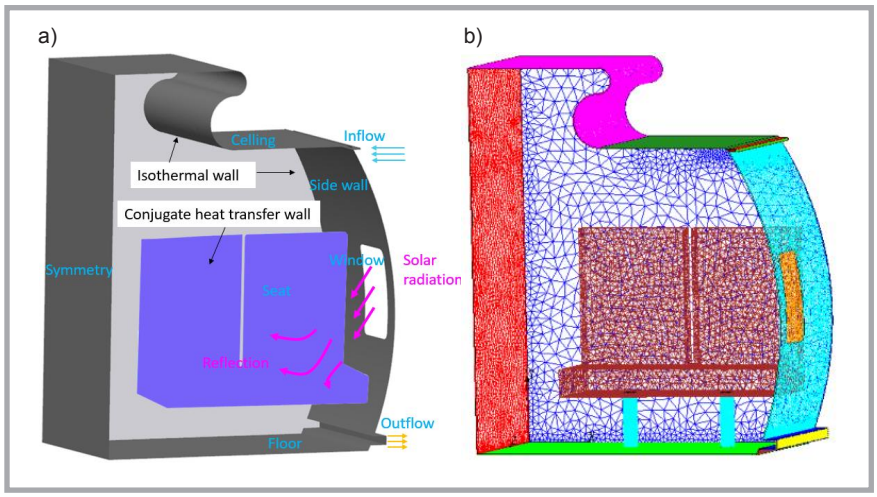

Figure 2. *Geometry model, boundary conditions and tetrahedral mesh: a) geometry model and boundary conditions, b) fluid zone mesh.*

reaches the cabin seat, and radiative heat transfer occurs between the airflow and seat fabric. In the process of light-ray propagation, a part of the light radiating to the seat is absorbed by the fabric, and another part is reflected to the air. At the same time, conductive heat transfer occurs between the heated seat and cooling air, and forced convective heat transfer occurs due to the air conditioner as well.

Physical modelling and grid generation

A steady numerical investigation was carried out on a three dimensional model of an aircraft cabin section. The transversal section of the aircraft geometric model is shown in ***Figure 2.a***. It was extruded by 2150 mm along the longitudinal axis and 1775 mm along the horizontal axis. ANSYS ICEM-CFD was used to obtain a three-dimensional tetrahedral mesh. To solve the near-wall heat flux correctly, the viscous effects at the wall must be considered. The normal grid spacing near the surface is particularly small to capture the detailed boundary layer. A grid independence analysis was performed and, for this purpose, different grids of 0.9 million (coarse), 1.5 million (moderate) and 2.0 million (refined) were tested [12]. The first grid spacing from the wall was chosen as 1×10^{-5} m to satisfy the y^+ criteria [13]. The y^+ over the entire wall surface is kept in the range of 0.8 to 1.2 on the cabin and fabric surface. Under this situation, the mesh that introduces acceptable errors, with respect to the refined grid tested, was selected to ensure accuracy of the computational results.

Governing equations and numerical procedure

The flow inside an aircraft cabin can be characterised as turbulent, weakly compressible flow containing both forced convection due to the air conditioning system, natural convection due to buoyancy and heat radiation due to solar radiation. This flow is modelled by the compressible Reynolds-averaged Navier-Stokes (RANS) equations, which are closed by the Realizable k-ε model [14, 15]. The conjugate heat transfer between the solid seat wall and the air flow is considered. The aluminum and air gas are identified as solid and fluid groups, respectively. In this situation, one equation set defines the equations of the fluid motion and another will define the equation for the thermal conduction in the solid [16]:

$$\vartheta\frac{\partial T}{\partial t}=K\left(\frac{\partial}{\partial x_i}\right)^2 T \qquad (1)$$

Where, ϑ represents the thermal capacitance and K – the thermal conductivity of the solid medium. They are 2427621 kg/(ms^{2}K) and 237.42 W/(mK) at a temperature of 293 K for pure aluminum. The heat exchange through radiation inside an aircraft cabin is governed by the radiative heat transfer equation. The radiative transfer equation (RTE) is integrated into each special finite volume element and finite solid angle element [17, 18]. The DO radiation model is employed here, which can include the effects of the particles on radiation. This particular model, which is often referred to as the finite volume radiation transfer method, is a variation of the standard DO method. In this model, the 4 angular space is discretised using finite solid angle elements, analogous to discretising the physical space using finite volume elements. The radiative transfer equation (RTE) is integrated over each the spacial finite volume element and finite solid angle element.

Consider the quasi-static radiative transport equation for an absorbing, emitting, and scattering gray medium which is at local thermal equilibrium. The RTE is

$$\nabla\left(I\hat{s}\right)=\kappa I^*\left(r\right)-\left(\kappa+\gamma\right)I\left(r,\hat{s}\right)+ +\frac{\gamma}{4\pi}\int_{\Omega=0}^{4\pi} I\left(r,\hat{s}'\right)\Phi\left(r,\hat{s}',\hat{s}\right)d\Omega \qquad (2)$$

where

$$I^*=\kappa\frac{\mathrm{n}^2\sigma T^4}{\pi} \qquad (3)$$

For isotropic scattering,

$$-k\frac{\partial T}{\partial\hat{n}_\omega}+\int_{4\pi} I\left(r,\hat{s}\right)\hat{s}\cdot n_\omega d\Omega=0 \qquad (4)$$

For linear anisotropic scattering,

$$\Phi(r,\hat{s}',\hat{s})=1+A_1(r)\hat{s}'\cdot\hat{s} \qquad (5)$$

Where, $A_1(r)$ is a coefficient independent of the directions.

For the Delta-Eddington phase function,

$$\Phi(r,\hat{s}',\hat{s})=2f\delta(1-\hat{s}'\cdot\hat{s})+ +(1-f)\Phi^*(r,\hat{s}',\hat{s}) \qquad (6)$$

Where, f is the forward scattering fraction, δ the Dirac delta function, and Φ^* is the base phase function, which can be a constant or a linear phase function, as described in ***Equation (5)***.

The first order differential term in RTE requires one boundary condition at the surface from which the radiation emanates. For a diffusely emitting and reflecting opaque enclosure, the intensity at location r_ω on the surface of the enclosure is

$$I(r_\omega,\hat{s})=\varepsilon I^*(r_\omega)+ +\frac{\chi}{\pi}\int_{n_\omega\hat{s}'>0} I(r_\omega,\hat{s})\, n_\omega\hat{s}'d\Omega' \qquad (7)$$

For opaque surfaces, the reflectance $\chi = 1 - \varepsilon$. In this paper, the emissivity and reflectance of the wall are 1.0 and 0. For the conjugate heat transfer of seats, an emissivity of 0.9 and a reflectance of 0.1 are used.

A system of governing equations, subject to their appropriate boundary conditions, was successfully solved by using the finite volume method. The equations are discretised in space by a second-order, cell-centered, finite-volume scheme for the basic flow equations. Computational analysis was performed by employing the commercial software CFD++ ver.14.1. The Courant number is set to less than 1 in order to ensure stability. Next, it can be increased to reduce the calculation time. The coupled-solver variable under-relaxation factor is set to 0.25. The convergence criterion is that the residual variations of the mass, momentum, and energy conservation equations become less than 10^{-4} [19]. The solution was obtained on an intel CORE i7 with eight 64 bit processors of 2.60 GHz each and 16 GB of RAM.

Boundary and initial conditions

The air inlet is based on boundary conditions, which assume an air inlet speed of 0.5 m/s, and the inlet temperature is 293 K. Set the base pressure level to 7.9×10^4 Pa, which corresponds to aircraft cabin pressure at cruise conditions. The gravitational acceleration vector is -9.81 m/s^2 for the gravity source, including the buoyancy effects. The bulk density is set to 0.9388 kg/(m^3). The solar rays enter into the cabin through the window positioned next to the passenger's shoulder, inclined at 45° to the vertical and horizontal. Hence, the window is set to be the radiative wall with constant properties and solar. The solar heat flux is 500 kg/s^3 and the solar direction (-0.707, -0.707, -0.707).

All boundaries except for the window are treated as a radiative wall with constant properties of the boundary condition. The solid walls of the floor, ceiling, and side wall in the aircraft cabin are all set to an isothermal-constant temperature of 297 K under non-slip conditions. The seat fabrics are treated as interfaces between the solid and fluid, and are set to be a conjugate heat transfer-fluid/solid with a wall function. The thermal conductivity and thickness of the seat are variable for different fabric.

Validation of numerical methods

The heat transfer of a two dimension model of natural convection and radiation in a square enclosure is used to validate the numerical method [20, 21].

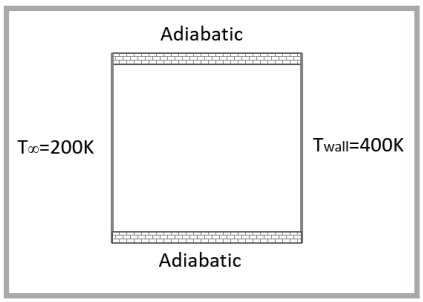

Figure. 3 *Natural convection and radiation in a square enclosure.*

The height and width of the enclosure is 1000 mm. The top and bottom walls are adiabatic. The left and right walls are kept at a constant temperature of 200 K and 400 K, respectively, as displayed in ***Figure 3***.

The wall heat fluxes are demonstrated in terms of a nondimensionalised coefficient (Nusselt number) [21], defined as

$$Nu=Q\times L/\left[k(T_{wall}-T_\infty)\right] \qquad (8)$$

The Nusselt numbers on the right boundary were calculated for all cases and are compared with the reference file. As shown in ***Table 2***, the numerical method used here can describe the convective and radiative heat flux accurately. Thus, it is satisfactory to carry out the following investigations.

Table 1. *Boundary conditions.*

Gravitational constant	g	9.81	m/s^2
Inflow velocity	v_∞	0.5	m/s
Inflow temperature	T_∞	293	K
Static pressure	p	79000	Pa
Bulk density	ρ	0.9388	kg/(m^3)
Specific heat at constant pressure	C_p	1005	J/(kg.K)
Solar heat flux	Q_{solar}	500	kg/s^3

Table 2. *Dimensionless average heat fluxes.*

Method	Yucel [19]		CFD	
	Total	Radiation	Total	Radiation
Nonradiating	13.76	0.00	13.69	0.00
DO radiation model	39.45	31.77	38.86	30.97

Table 3. *Calculation conditions with different fabric materials and thicknesses.*

	Materials	Thermal conductivity, W·m^{-1}·K^{-1}	Thickness, m	Specifc heat, J·kg^{-1}·K^{-1}	Density, kg·m^{-3}
Case 1	Polar fleece	0.028	0.001	1340	159.17
Case 2	Cotton and foaming	0.10	0.001	1220	364.42
Case 3	Carbon fibre yarn	0.528	0.001	1318	1789.9
Case 4	Cotton and foaming	0.10	0.007	1220	364.42
Case 5	Cotton and foaming	0.10	0.015	1220	364.42

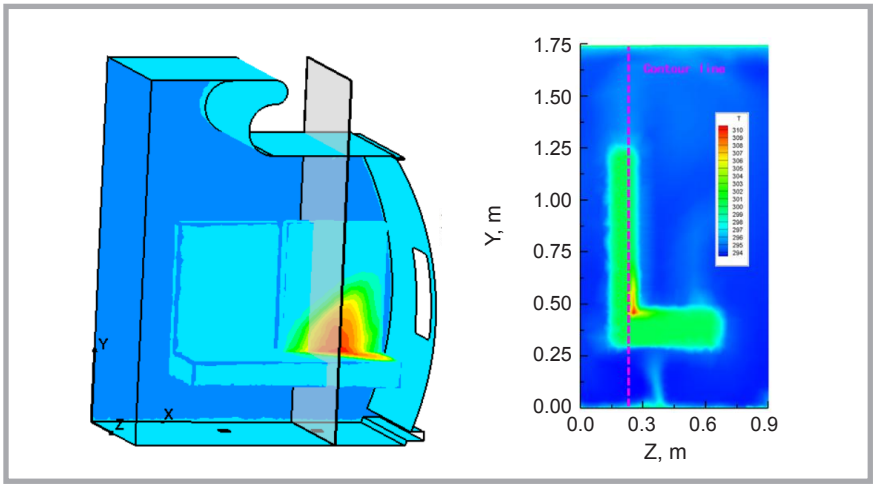

Figure 4. Cutting plane of x = 1.2 m and contour line of z = 0.25 m.

Table 4. Peak value of temperature and heat flux.

	Temperature on seats, K	Radiative heat flux on seats, W/m^2
Case 1	304.45	214.52
Case 2	299.98	229. 31
Case 3	298.58	235.19
Case 4	312.05	197.54
Case 5	318.91	171.66

Results and discussions

In order to simulate different conditions of the cabin–fabric–environment, five kinds of simulation were carried out. The seat padding was simulated with three kinds of textiles [11, 22] of different thickness, as in ***Table 3***.

Temperature and heat transfer distribution

To clarify the characteristic features of the thermal seat climate, the flow parameter distribution results will be explained in detail in the following paragraphs. ***Table 4*** gives the peak value of the temperature and heat flux on the surface of cabin seats. When considering cases 1, 2 and 3, we can observe that the peak temperature and heat flux vary with the changing of seat materials. The maximum temperature on the seat is 304.45 K and the peak value of radiative heat flux is 214.52 W/m^2 when the fabric is polar fleece. The peak of the temperature decreases by about 1.5% and the heat flux increases by 6.9% when changing to cotton and foaming.

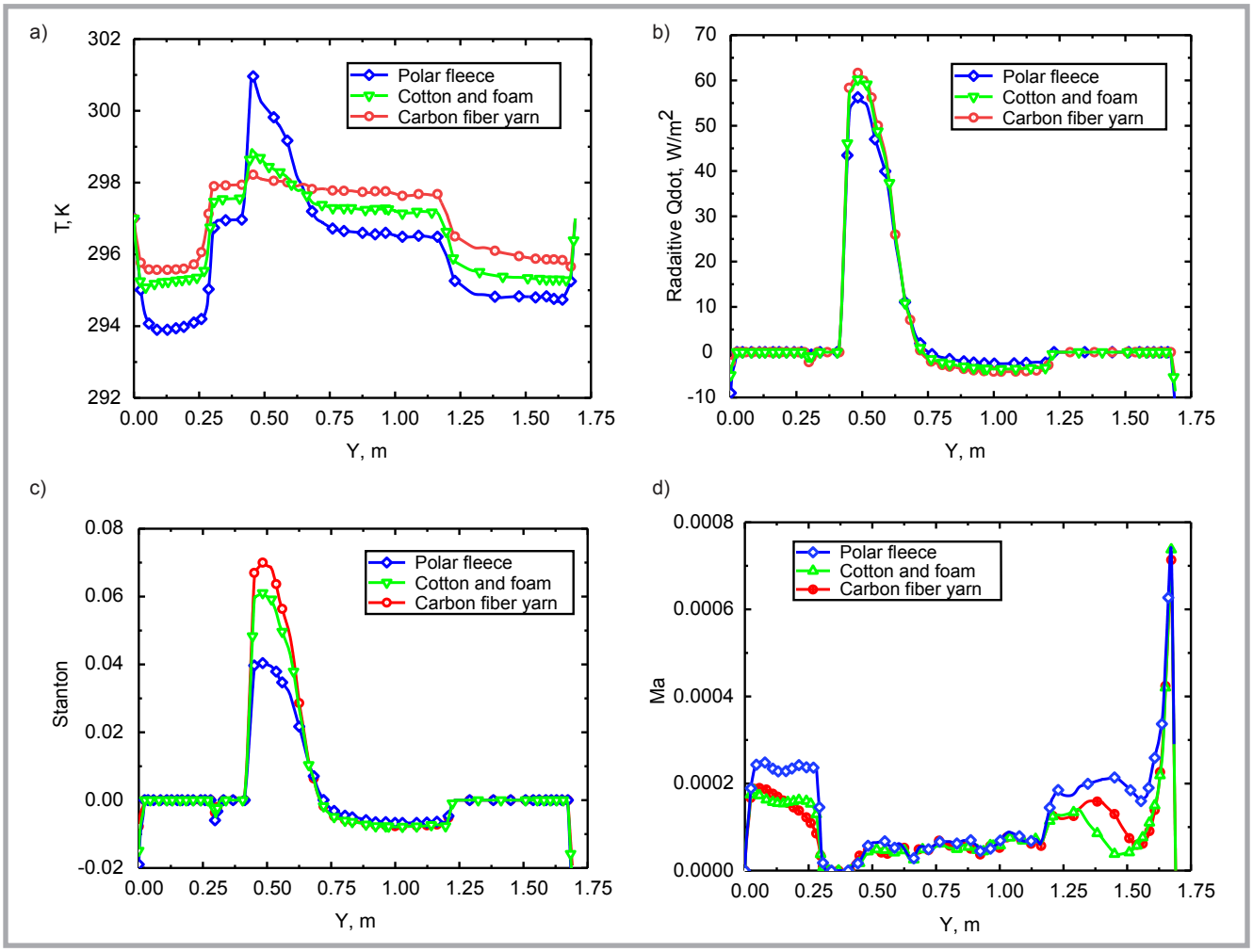

Figure 5. Contour distributions on x = 1.2 m, z = 0.025 m with different fabrics: a) temperature distribution, b) radiative heat flux distribution, c) Stanton number distribution, d) Mach number distribution.

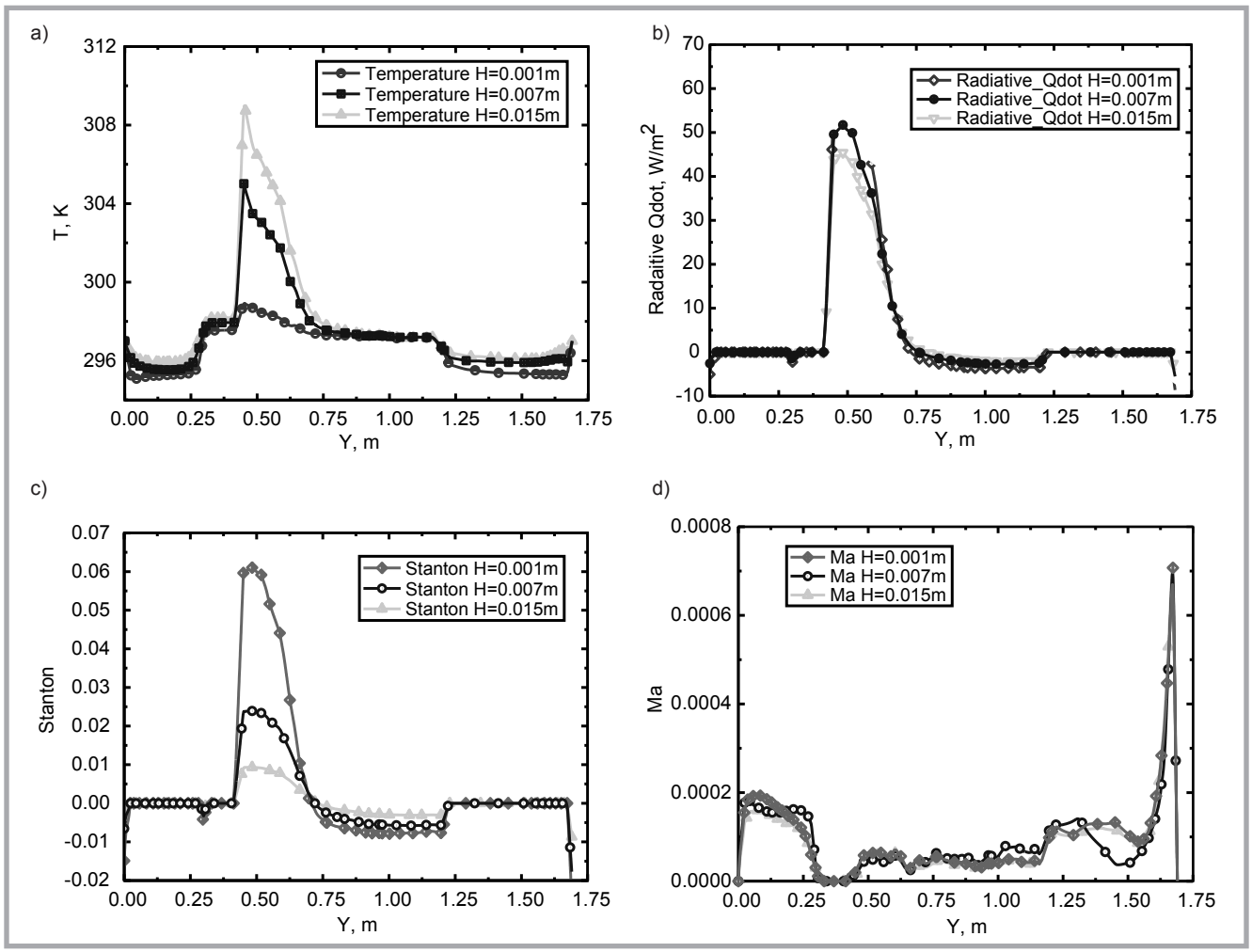

Figure 6. *Contour distributions on x = 1.2 m, z = 0.025 m with different cushion thicknesses: a) temperature distribution, b) radiative heat flux distribution, c) Stanton number distribution, d) Mach number distribution.*

These peak values continue to change by about -1.9% and 9.6% when changing to carbon fibre yarn.

Temperature and heat transfer of different fabrics

Various types of fabric of different thermal conductivity and constant thickness H = 0.001 m are considered, namely cases 1, 2 and 3. The thermal conductivities of these materials are 0.028, 0.10 and 0.528. In order to compare the flow parameters for different cases, a fixed contour line of the cabin section is selected at the location of x = 1.2 m, z = 0.025 m, as shown in ***Figure 4***.

The cabin seat surface heat transfer is demonstrated in terms of the dimensionless coefficient known as the Stanton number [10], defined as

$$St=Q/\left[v_{\infty}\rho_{\infty}C_{p}(T_{wall}-T_{\infty})\right] \qquad (9)$$

A comparison of the temperature, heat transfer and Ma number distributions on the line of x = 1.2 m, z = 0.025 m is shown in ***Figure 5.*** As can be seen in ***Figure 5.a***, the temperature remains at the low level of lower than 296 K, near the area of air inflow and outflow. However, it increases to a high level on the surface of cabin seats, with even a peak appearing at the juncture of the horizontal and back cushion. ***Figures 5.b*** and ***5.c*** show that carbon fibre yarn yields the highest radiative heat flux on the seat surface, and brings about the greatest value of the dimensionless heat transfer coefficient – the Stanton number. It can be seen from the comprehensive ***Figures 5.a***, ***5.b*** and ***5.c*** that the lower the thermal conductivity of the fabric, the higher the temperature on the surface. Polar fleece leads to a higher temperature gradient. The carbon fibre yarn seat has a more comfortable environment than the others. ***Figure 5.d*** compares the Mach number distributions in the line, showing that polar fleece leads to a bigger air velocity than the other two. The reason is that the large temperature gradient brings natural convection, then increases the air velocity nearby.

Temperature and heat transfer of different thicknesses

In order to investigate the influence of fabric thickness, cabin seat padding made of cotton and foaming with a constant thermal conductivity of 0.01 was analysed. The thickness varies from 0.001 m, 0.007 m to 0.015 m. The temperature, heat transfer and Ma number distributions in the line of x = 1.2 m, z = 0.025 m are shown in ***Figure 6***. As shown in ***Figure 6.a***, the temperature on the seat surface increased with the fabric thickness, with the case of H = 0.15 m having a higher temperature level than the others. ***Figures 6.b*** and ***6.c*** depict that the radiative heat flux and transfer heat flux in the case of H = 0.015 m are lower than the others. Thus, it can be concluded that the thicker the cushion fabric, the higher the temperature on the seat surface. This phenomenon can be explained

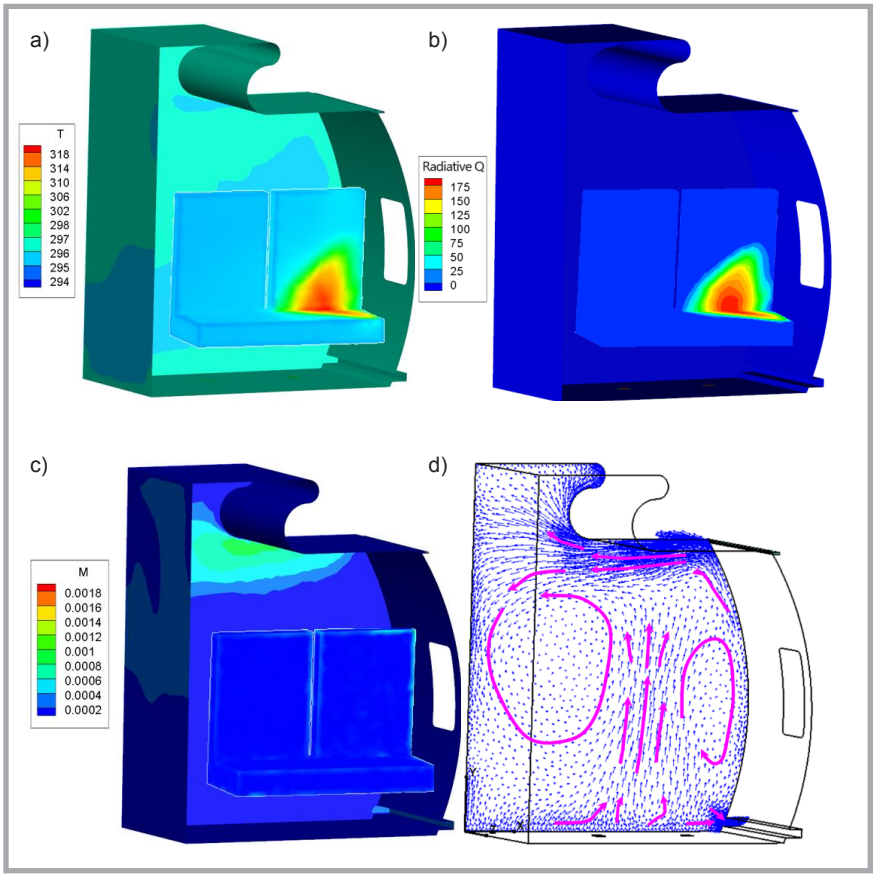

Figure 7. *Contours of cabin flowfield: a) temperature contours, b) radiative heat flux contours, c) Mach number contours, d) velocity vectors on xoy plane.*

by the fabric becoming thicker and the heat transfer ability becoming weaker. As can see in ***Figure 6.d***, the Mach number behaves very similarly with different thicknesses, with only a little difference in the inflow and outflow area.

Flow contours and mechanism analysis

In order to examine the flow mechanism, the flow contours of the cabin were analyzed. ***Figure 7*** shows the typical flow field of case 4. ***Figure 7.a*** shows that there appears a large temperature gradient on the surface of the first seat near the window because of the solar radiation. Meanwhile, the temperature gradient is bigger near the wall because of the outward heat loss of the wall. ***Figure 7.b*** depicts that the cabin seat reflects parts of the solar radiative heat flux from the radiative wall. Other walls emit heat flux without reflection. ***Figure 7.c*** shows that the air velocity is much bigger near the inflow area, and tends to be uniform in other areas. The velocity vectors on the *xoy* plane can be seen in ***Figure 7.d***, showing that the cooling air flows from the inflow entrance to the outflow exit and forms a double circular pattern in the cabin. This phenomenon agrees well with the Mach number contours. The circulation of air can improve the thermal environment partly.

Concluding remarks

The primary goal of the present paper was to investigate several important thermal issues in a section of an aircraft with the three-dimensional finite volume method. Special attention was given to understanding the solar radiation and conjugate heat transfer on the seat textile. The effect of the fabric type and textile thickness was obtained. Some conclusions can be drawn based on the results:

(1) The comparison of the temperature for three different textiles shows that different types of fabric yield different temperature distributions on the seat and that polar fleece brings the highest peak temperature. Carbon fibre yarn yields the highest radiative heat flux on the seat surface and brings about the greatest value of heat transfer.

(2) The comparison of temperature for different textile thicknesses varying from 0.001 m to 0.007 m and 0.015 m shows that the thickest pad brings a lower radiative heat flux and transfer heat flux than the others. As a result, this type of padding obtains the highest the temperature on the seat surface.

(3) The velocity vectors and Mach number distribution in the flowfeild show that proper selection of materials, thicknesses and air flow circulations ensure the thermal comfort of the passenger.

However, more work is needed to be done in order to investigate the effect of the air flow velocity, the angle between the air flow and the fabric and the insulation method for solar radiation.

References

1. Kok JC, Muijden JV, Burgers SS. Enhancement of Aircraft Cabin Comfort Studies by Coupling of Models for Human Thermoregulation, Internal Radiation, and Turbulent Flows. *European Conference on Computational Fluid Dynamics*, TU Delft, The Netherlands, 2006; 1:1-18.
2. Kovačević S, Domjanić J, Pačavar S. Effects of Layer Thickness and Thermal Bonding on Car Seat Cover Development. *FIBRES & TEXTILES in Eastern Europe* 2017; 25, 2(122): 76-82. DOI: 10.5604/12303666.1228186.
3. Angelova Radostina A. *Textiles and Human Thermophysiological Comfort in the Indoor Environment*. CRC Press, 2015; 10: 15-33.
4. Bhattacharjee D, Kothari VK. Prediction of Thermal Resistance of Woven Fabrics. Part II: Heat Transfer in Natural and Forced Convective Environments. *Journal of the Textile Institute* 2008; 99(5), 433-449.
5. Günther G, Bosbach J, Pennecot J, et al. Experimental and Numerical Simulations of Idealized Aircraft Cabin Flows. *Aerospace Science & Technology* 2006; 10(7), 563-573.
6. Kühn M, Bosbach J, Wagner, C. Experimental Parametric Study of Forced and Mixed Convection in a Passenger Aircraft Cabin Mock-up. *Building & Environment* 2009; 44(5), 961-970.
7. Hu Z, Wang L, Wang H, et al. Heat Transfer Based Numerical Investigation of Aircraft Cabin Environment from Various Inlet Conditions. *Frontiers in Heat and Mass Transfer* 2015; 6(1): 17-25.
8. Maier JM, Micheel CM. Ceiling-Based Cabin Displacement Ventilation in an Aircraft Passenger Cabin: Analysis of Thermal Comfort. *Building and Environment* 2018; 146: 29-36.
9. Khalil EE, Kotb H. Numerical Simulation of Airflow and Airborne Pathogen Trans-

port in Aircraft Cabins: Dynamic Mesh Analyses. *AIAA Scitech 2020 Forum*, 2020; 1: 1-9.
10. Dehne T, Bosbach J. Transient Temperature Fields of Turbulent Mixed Convection in an Aircraft Cabin Caused by a Local Heat Source. *Notes on Numerical Fluid Mechanics and Multidisciplinary Design* 2016; 132: 371-381.
11. Zhu G, Kremenakova D, Wang Y, et al. 3D Numerical Simulation of Laminar flow and Conjugate Heat Transfer through Fabric. *Autex Research Journal* 2017; 17(1): 53-60.
12. Jia J, Fu D, He Z. Aerodynamic interactions of a Reusable Launch Vehicle model with different nose configurations. *Acta Astronautica*; 2020; 177: 58-65. DOI: 10.1016/j.actaastro.2020.07.022.
13. Jia JH, Zhang YJ. Heat Flux and Pressure Reduction Using Aerospike and Counterfowing Jet on Complex Hypersonic Flow [J]. *International Journal of Aeronautical and Space Sciences* 2020; 21(2): 337-346.
14. Maślanka P, Korycki R. Textile Cover Effect on Aerodynamic Characteristics of a Paraglider Wing. *FIBRES & TEXTILES in Eastern Europe* 2019; 27, 1(133): 78-83. DOI: 10.5604/01.3001.0011.7511.
15. Jin Y, Zhu S, Cui J, Li J, Zhu Z. Investigating the Effect of the Opening Unit on the Airflow Field in Rotor Spinning. *FIBRES & TEXTILES in Eastern Europe* 2017; 25, 5(125): 18-24. DOI: 10.5604/01.3001.0010.4622.
16. Incropera, Frank P, DeWitt, et al. *Introduction to Heat Transfer Fourth Edition*, John Wiley & Sons, New York, 2002: 265-266.
17. Modest MF. *Radiative Heat Transfer*, Academic Press, 2nd edition, San Diego, 2003: 55-73.
18. Metacomp Technologies Inc. CFD++ User Manual, Agoura Hills, CA. 2013.
19. Yang R, Gao W, Xue Y. Airflow Characteristics During the Rotor Spun Composite Yarn Spinning Process. *FIBRES & TEXTILES in Eastern Europe* 2017; 25, 5(125): 13-17. DOI: 10.5604/01.3001.0010.4621.
20. Yucel A, Acharya S, Williams ML. Natural Convection and Radiation in a Square Enclosure. *Numerical Heat Transfer, Part A*.1989; 15: 261-278.
21. Minovski B, Lofdahl L, Gullberg P. Numerical Investigation of Natural Convection in a Simplified Engine Bay. *SAE 2016 World Congress and Exhibition* 2016; 1-9.
22. Serweta W, Olejniczak Z, Woźniak B. Analysis of Insole Material Impact on Comfort During Physical Exertion. *FIBRES & TEXTILES in Eastern Europe* 2018; 26, 2(128): 100-103. DOI: 10.5604/01.3001.0011.5746.

Received 04.02.2020 Reviewed 27.05.2020